ELSEVIER

Journal of Nuclear Materials 298 (2001) 248–254

journal of nuclear materials

www.elsevier.com/locate/jnucmat

Mechanical properties of pure tantalum after 800 MeV proton irradiation

J. Chen [a,*], H. Ullmaier [a], T. Floßdorf [a], W. Kühnlein [a], R. Duwe [a], F. Carsughi [b], T. Broome [c]

[a] *Projekt ESS, Forschungszentrum Jülich, D-52425 Jülich, Germany*
[b] *DIBIAGA, University of Ancona, I-60131 Ancona and INFM Unitá di Ancona, Italy*
[c] *Rutherford Appleton Laboratory, Chilton, OX 11 0QX, UK*

Received 7 May 2001; accepted 9 July 2001

Abstract

Specimens prepared from a spent tantalum target of the pulsed spallation source ISIS, irradiated with 800 MeV proton to a maximum fluence of 1.7×10^{25} p m^{-2} at temperatures lower than 200 °C, were investigated by microhardness, three-point bending and tensile tests at room temperature (RT) and at 250 °C. All three types of mechanical measurements consistently showed irradiation hardening. Furthermore, the tensile tests showed that the increase in yield strength is accompanied by a reduction of the strain-to-necking at both test temperatures. For instance, at RT, the strain-to-necking was reduced by irradiation from initially 30% to about 10%. This drop in ductility occurred at doses below 0.6 dpa, whereas afterwards the strain-to-necking remained constant up to the maximum dose of about 11 dpa. The results of tests at 250 °C were similar to those at RT. SEM investigation revealed typical ductile fracture surfaces even for the highest doses. Optical micrography after bending tests showed no cracks even after bending of a 2 mm thick specimen end to end, indicating that pure Ta retained very high ductility after proton irradiation.

PACS: 61.80; 81.40

1. Introduction

The lifetime of the structural target components of spallation neutron sources and accelerator-driven systems (beam window, liquid metal container, return hull, etc.) is determined by irradiation-induced changes of their mechanical properties. Up to now, only scarce information has been available on the behaviour of candidate materials under such conditions: high radiation damage levels, very high rates of helium and hydrogen generation, and relatively low irradiation temperatures. Typically, the target window of the planned European Spallation Source (ESS) [1] will accumulate a maximum proton fluence of $1.6 \times 10^{26}/\text{m}^2$ within one year of full power operation. In steels, e.g., this leads to a displacement dose of about 60 dpa and 1 at.% helium [2]. To build up a spallation materials database, we therefore initiated an extensive test programme based on the investigation of specimens obtained from spent target components of operating spallation sources (LANSCE, Los Alamos National Laboratory and ISIS, Ruthford–Appleton-Laboratory). Four different classes of materials are investigated, including a nickel-based alloy (Inconel 718), an austenitic stainless steel (AISI 304L), a martensitic stainless steel (DIN 1.4926) and a refractory metal (tantalum). The preliminary results for AISI 304L, DIN 1.4926, and Inconel 718 have been published [3–5]. Here the results on pure tantalum (99.99%) from a spent target of the ISIS facility are reported.

* Corresponding author. Tel.: +49-2461 612 473; fax: +49-2461 614 413.
E-mail address: j.chen@fz-juelich.de (J. Chen).

0022-3115/01/$ - see front matter
PII: S0022-3115(01)00654-7

2. Experimental

The ISIS target consists of a window made of 304L stainless steel and 23 water-cooled Ta plates with 90 mm in diameter and thicknesses ranging from 7.7 to 26.2 mm. The high purity tantalum for the plates was supplied by Plansee GmbH, Austria. It had been cold rolled with intermediate annealing at 1280 °C and finally annealed at 1200 °C for 2 h. The metallography showed equiaxed grains with a mean size of about 50 μm and only a few grains with sizes as big as 300 μm. The maximum values of the impurity levels quoted by the supplier and by our IR-spectroscopy and atom-spectroscopy analysis are listed in Table 1.

During service in the period 1988–1994, the target was irradiated with a pulsed 800 MeV proton beam (pulse length 0.5 μs, repetition frequency 50 Hz) at temperatures lower than 200 °C. The total accumulated number of protons incident on the target was 3.9×10^{22}. To identify the profile of the proton beam on the spent ISIS target, γ-scans were performed on the beam window of the target in the hot cells of FZ-Jülich. It was found that positron decay of Na^{22}, Ti^{44}, Co^{57}, etc. was mainly due to the proton beam. Therefore the integrated positron decay distribution was used to obtain the proton beam profile, giving a two-dimensional Gaussian distribution with horizontal and vertical variances of $\sigma_x = (17.0 \pm 0.2)$ mm and $\sigma_y = (20.7 \pm 0.4)$ mm, respectively (see Fig. 1). These values together with the total number of protons result in a maximum fluence of 1.7×10^{25} p m^{-2}, corresponding to one-tenth of a year of full power operation of ESS. Taking for Ta a displacement damage cross-section and He-production cross-section of 6650 and 0.342 b, respectively, [6], the maximum displacement dose and helium concentration should be 11.3 dpa and 580 at. ppm, respectively. The cross-sections used here are lower than those calculated earlier by the code HETC [7–9] which overestimates the helium production cross-section when compared to measured values. It should be noted that the neutron contribution to displacement damage and He production is not included in the above numbers.

For sample preparation, two 2.5 mm wide strips of A and B were first cut from the Ta plate closest to window (No. 1 with thickness of 7.7 mm) along the vertical direction close to the centre of the proton beam (marked in Fig. 1). Before cutting strip A into bending samples, Vickers micro-hardness tests were performed on the cut and polished surface as a function of the position along the strip. To examine possible differences along beam direction, the micro-hardness was also measured close to the front side and back side of the plate. However, no difference could be detected, indicating that the temperature distribution along beam direction, i.e., across the plate thickness, had no effect on the mechanical properties. Afterwards, the strip A was cut into bending samples, 15 mm long, 2.5 mm wide and 2.0 mm high. The reason for this unusual geometry of bending samples was to keep the dose variation in each specimen small and to have a sufficient number of specimens for studying the dose dependence. The three-point bending tests were performed with a cross-head speed of 0.2 mm/

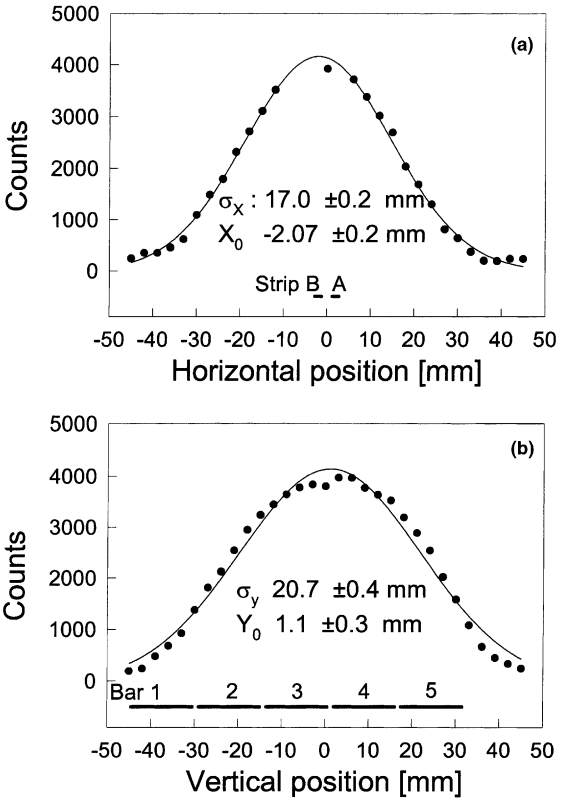

Fig. 1. Two-dimension Gaussian distribution of the 511 keV γ-intensity reflecting the proton beam profile on the ISIS target. (a) and (b) are the distributions of 511 keV γ along short and long axes, respectively. The solid lines are the best fits. The sample cutting is illustrated by the vertical strips and horizontal bars. The origin of the coordinate system coincides with the geometrical centre of the target.

Table 1
Maximum concentrations of main impurities in pure tantalum (wt% ppm)

Element	C	N	O	Zr	W	Nb	Mo	Hf	Others	Ta
Quoted	30	5	40	1	20	400	10	5	117	>99.99 (wt%)
Analysed	20	6	8	5	10	10	2	5	–	>99.99 (wt%)

min at room temperature (RT) (the bending device is described in 3). Strip B was used to machine tensile samples. For the same reason, miniature-type dog-bone tensile specimens were used in the present study, i.e., strip B was cut into bars of 15 mm length and then slices of about 0.7 mm thickness were cut from the bars. After machining them to a dog-bone shape, the surfaces of the slices were polished. Finally, tensile samples with 0.5 mm thickness, 5 mm length and 1.2 mm width in the gauge area were obtained. The tensile tests were performed at RT and 250 °C, respectively, using a 2 kN MTS tensile machine equipped with a video-extensometer so that the elongation could be measured directly in the gauge area. The strain rate was about 10^{-3} s^{-1}. After tensile testing, the fracture surfaces were investigated by scanning electron microscopy to identify the fracture mode.

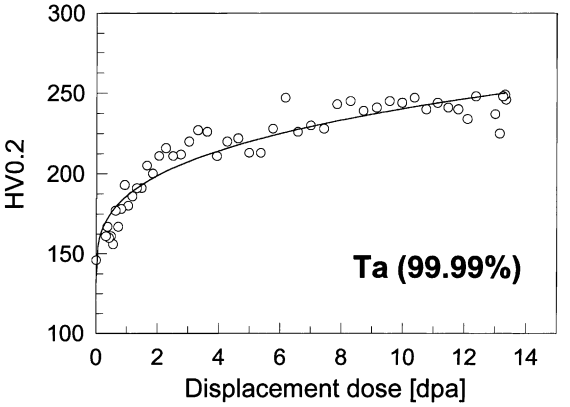

Fig. 2. Dependence of Vickers micro-hardness HV0.2 at RT on displacement dose.

3. Results

The first tests conducted were micro-hardness measurements since they are easy to perform and provide a quick qualitative information on the changes of mechanical properties. The results given in Fig. 2 show the expected increase of the hardness with dose. The subsequent bending tests confirmed the hardening but moreover indicated high ductility because none of the specimens failed within the maximum available bending deflection of 2.0 mm. Even bending an irradiated specimen end to end did not lead to rupture (Fig. 3(a)) and optical micrography of its tensile region did not reveal any cracks (Fig. 3(b)). This finding came as a surprise because earlier results on less pure and alloyed Ta [10,11] showed drastic embrittlement already at very low doses.

Therefore, in order to quantify our bending results, we performed tensile tests at RT and 250 °C, respectively. This is the temperature range of operations for structural materials in spallation sources employing liquid mercury targets, such as ESS or its US pendant SNS under construction in Oak Ridge. Fig. 4 gives the stress–strain curves for three typical doses. At RT the unirradiated specimens show a sharp yield point followed by slight work hardening and strains-to-necking of 30%. Irradiation causes significant strengthening and a reduction of strain to necking down to about 10%. This drop in ductility occured at doses below 0.6 dpa without a further decrease up to the maximum available dose of 11 dpa (Fig. 5). A similar behaviour was found for the test temperature of 250 °C. Here, the slight work softening of the irradiated samples (Fig. 4(b)) made it difficult to specify the ductility precisely. We defined the strain-to-necking as the strain at which stress started to drop rapidly. This was also the point where visible necking was observed in the video-extensometer. It is known from other work that under condition of localized deformation, engineering stress decreases without necking [12].

After tensile testing, the fracture surfaces were examined by scanning electron microscopy to identify the fracture mode. The fracture morphologies of the samples after testing at RT and at 250 °C are shown in Figs. 6 and 7, respectively. A wedge-shaped neck is formed during failure of the reference material with almost 100% reduction of area at both test temperatures. An example is given in Fig. 6(a). The reduction of area decreased with increasing displacement dose. For tests at RT, reductions in area are 100% for 0 dpa, 70% for 8.5 dpa and 56% for 11 dpa. In all cases a rough dimpled fracture surface was observed, characteristic of a ductile transgranular fracture mode. The only exception was a specimen irradiated to 11 dpa which, besides overall necking, also exhibited 'necking' of individual grains (Fig. 6(b)), sometimes up to the formation of sharp wedges (Fig. 6(c)) before rupturing with the usual rough dimpled surface (Fig. 6(d)). For the samples tested at 250 °C, the reductions in area are 100% for 0 and 0.6 dpa, 95% for 3.3 dpa and 61% for 11 dpa. The fracture surfaces (Fig. 7) show the same features as those observed for the RT tested specimen, indicating ductile transgranular failure also at the higher test temperature.

4. Discussion and conclusion

The steels developed in the European fusion programme, austenitic AISI 316L, and ferritic-martensitic MANET, are also candidate materials for the Hg-container, safety hull and proton beam window in ESS and SNS. However, both types of materials exhibit deterioration which may limit their lifetime in high-power spallation targets to rather low values. For

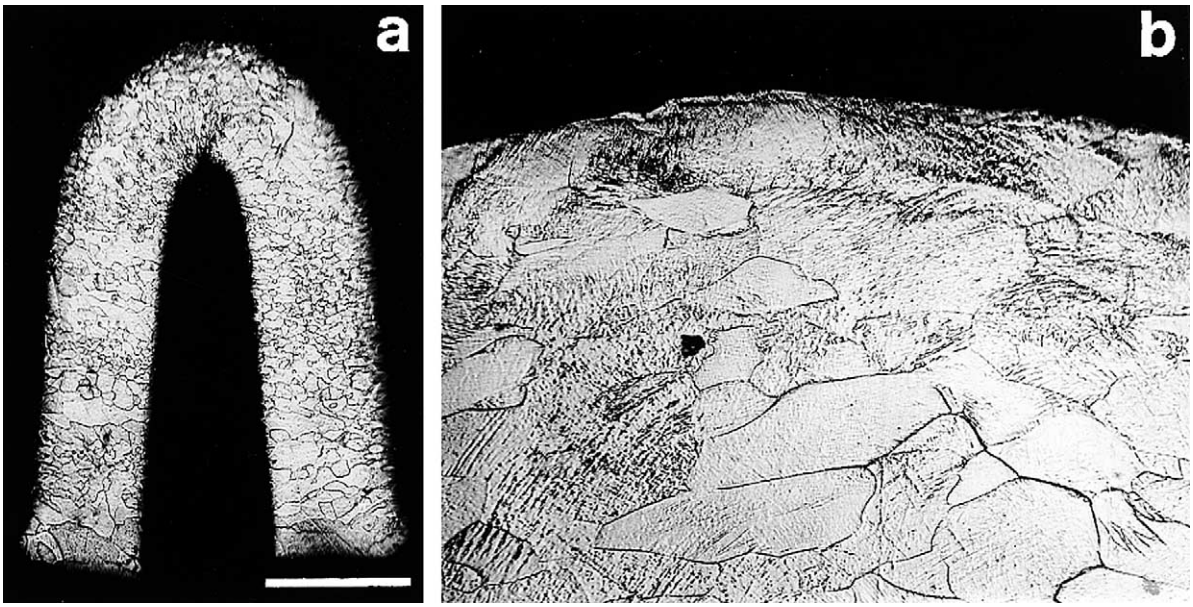

Fig. 3. Optical micrographs of a sample irradiated to 10 dpa after bending end to end. The scale in the photo indicates 2 mm and 0.2 mm for (a) and (b), respectively.

example, in AISI 304L intergranular failure covering about 60% of the total fracture surface was found already below 8 dpa [5]. Moreover, the uniform elongation approached zero in 160 °C tensile tests on AISI 304L and 316L [13] at even lower dose levels. The martensitic steels EM 10 and T 91 were found to fail in the elastic range after implantation of 0.5 at.% helium [14]. On the other hand a LAMPF beam window made from Inconel 718 did not fail within a service time corresponding to 20 dpa, although post-irradiation test revealed zero ductility [15]. Which kind of impact such findings will have on the use of these materials in

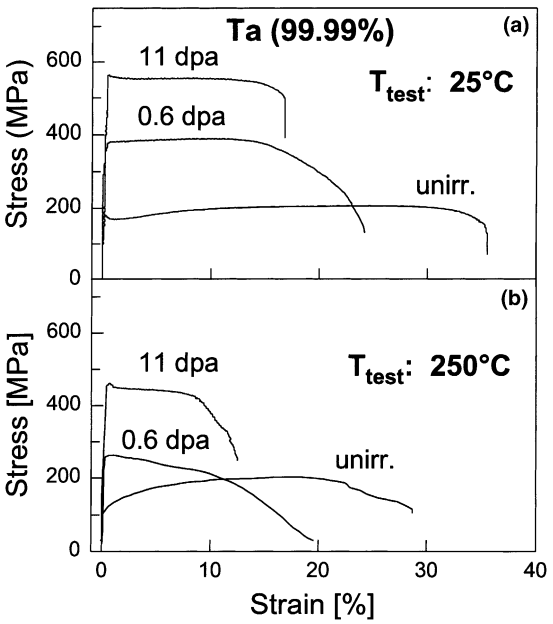

Fig. 4. Stress–strain curves of Ta specimens: (a) tensile tested at RT with a strain rate of 10^{-3} s^{-1}; (b) tensile tested at 250 °C with a strain rate of 10^{-3} s^{-1}.

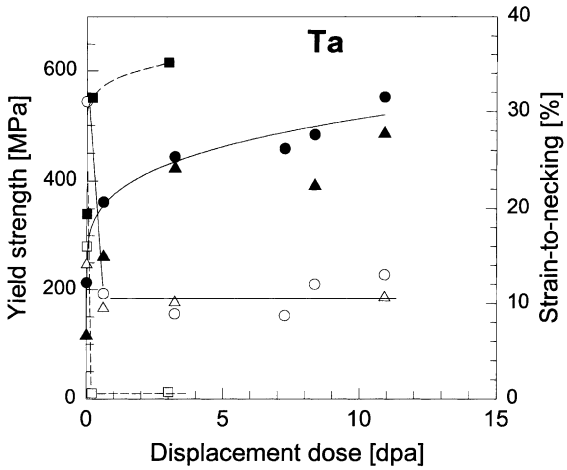

Fig. 5. Yield strength (filled symbols) and strain-to-necking (empty symbols) as a function of the displacement dose for Ta. The circles and triangles indicate the present results of high pure tantalum tested at RT and 250 °C, respectively, the squares indicate data for impure tantalum (from [10]). The solid and dashed lines serve as a guide to the eye.

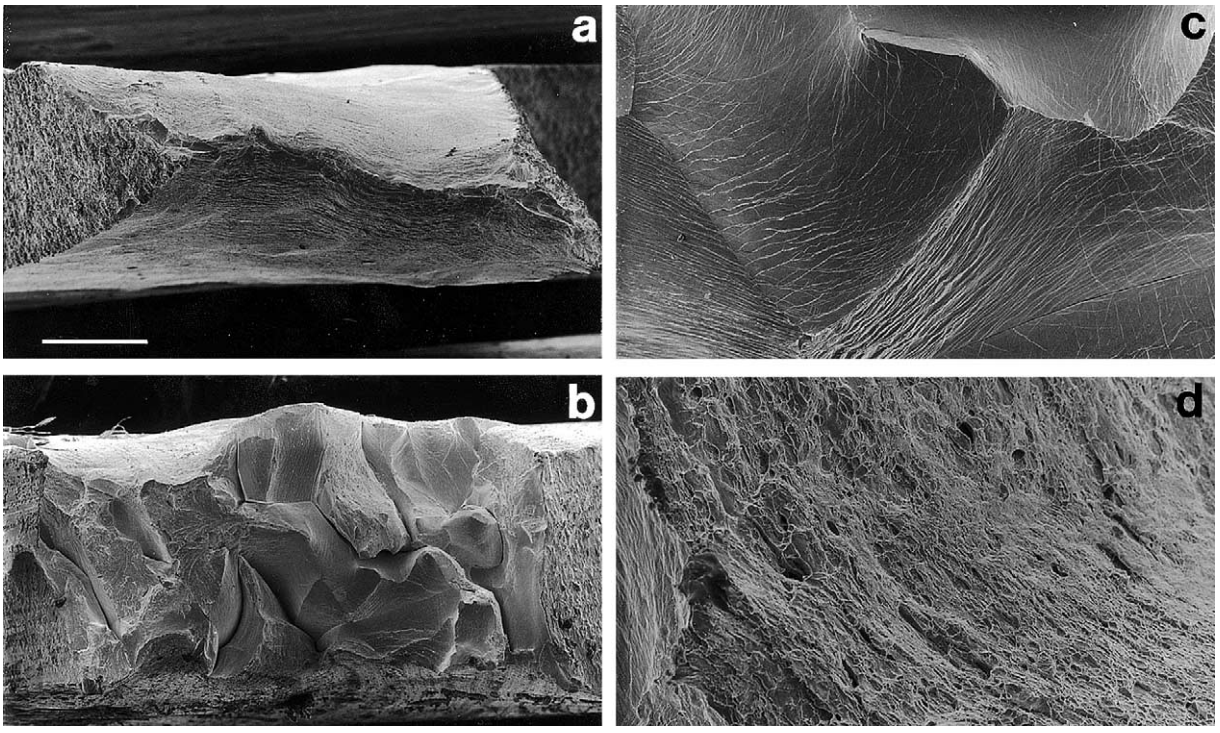

Fig. 6. Scanning electron micrographs of the fracture surfaces of tantalum specimens tensile tested at RT, (a) unirradiated sample, (b) sample with 11 dpa, (c) an enlarged part of (b), showing individual grain-necking (d) an enlarged part of (b), showing a rough dimpled fracture surface. The scale in the photo indicates 250, 250, 40 and 20 μm for (a), (b), (c) and (d), respectively.

spallation target technology depends on the engineering design criteria which are not yet clearly determined for the spallation case.

Nevertheless, it is desirable to extend the present palette of candidate materials. The present results suggest that pure Ta is such a promising alternative. Similar as that found in martensitic steels, irradiation of Ta to a few tenth that of a dpa decreases its ductility which then remains constant up to the maximum available dose of 11 dpa (Fig. 5). However, the 'saturation' strain-to-necking in martensitic steel is less than 1.5% [4] whereas it remains around 10% for Ta. A possible criterion for the use of structural materials is their toughness. A qualitative measure of this parameter is the area under the stress–strain curve, the so-called tensile toughness. For Ta, the relatively moderate drop in irradiation-induced ductility is compensated by the strength increase, leading to a practically irradiation-independent tensile toughness (Fig. 8). Its small absolute value (80 and 50 MJ/m^3 for RT and 250 °C, respectively) is due to the low initial strength of pure Ta (Figs. 4 and 5), an apparent disadvantage which the materials share with annealed austenitic steels. However, tantalum has a low thermal expansion coefficient and a high thermal conductivity. Therefore, its resulting thermal stress coefficient which determines the thermal stress loads on a material is 15 and 3.5 times lower than for austenitic steels and ferritic-martensitic steels, respectively.

Besides its favourable thermomechanical properties and resistance to irradiation embrittlement, pure tantalum has excellent corrosion resistance, especially also to mercury up to 600 °C [16]. In spite of these prospects, a full evaluation of the potential of Ta as a superior structural material for spallation targets cannot be done before proving that the saturation of irradiation-induced changes of mechanical properties is maintained to dose levels which considerably exceed the values available up to now.

At present it is not clear why the ductility of irradiated Ta remains high whereas earlier experiments [10,11] showed drastic embrittlement already at very small doses. Two possible reasons have been discussed. Firstly, it could be suspected that the protons in ISIS, bundled into extremely short pulses (0.5 μs), are less effective than the long pulses (1 ms) of LAMPF [10] and the continuous flux of reactor neutrons [11]. However, a careful theoretical analysis [17] rules out any pulsing effects on radiation damage in the spallation-relevant parameter ranges. An experimental verification will soon be available by comparing the results on spent targets (pulsed irradiation [3–5] and present work) with the

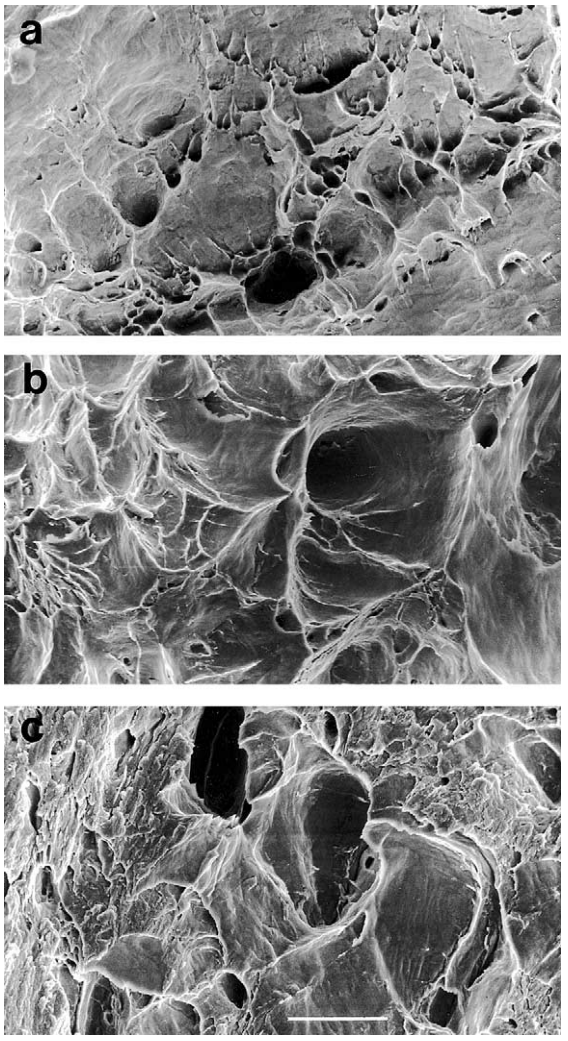

Fig. 7. Scanning electron micrographs of the fracture morphology of tantalum specimens tensile tested at 250 °C, (a) 0.6 dpa, (b) 3.3 dpa and (c) 11 dpa. The scale in the photo indicates 4 μm.

continuously irradiated specimens from the STIP-Programme. [1]

A more likely reason for the discrepancy of the present results with those of [10,11] is the different purities of specimens. Whereas the total impurity content of Ta in the ISIS target is less than 100 wt% ppm (Table 1), the 'technical' Ta used in [10,11] usually contains high concentrations of interstitial impurities (C, N, O) picked up during heat treatments in poor vacuum. This difference is reflected in the yield stress of the unirradiated materials: 210 MPa for the pure material and 340 MPa for the material of [10]. In an international collaboration (FZ-Jülich, Los Alamos and Oak Ridge Nat. Labs., Paul–Scherrer-Institut) experiments are under way to clarify the synergistic effects of radiation damage and impurities on the ductility of tantalum. In addition, TEM investigations of specimens from the ISIS target are in progress to correlate the changes of the mechanical properties with the underlying microstructure. Finally, cyclotron experiments for studying helium effects are planned at FZ-Jülich.

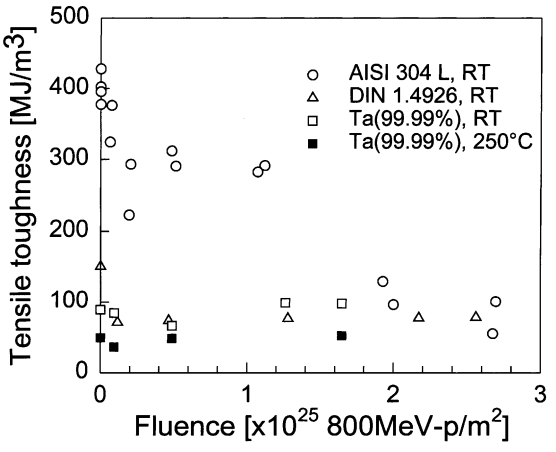

Fig. 8. Comparison of the tensile toughness of austenitic steel AISI 304L, martensitic steel DIN 1.4926 and high purity tantalum as a function of proton fluence. For lifetime considerations the proton fluence is a more meaningful parameter than the dpa number because the displacement cross-section of Ta is higher than for steels.

It is anticipated that the results of these investigations and their analysis will allow well-founded extrapolations of the irradiation behaviour of tantalum to higher doses. However, a safe prediction of its lifetime as structural material in the 5 MW ESS target which would also be accepted by licensing authorities will require irradiation experiments to the desired dose levels of about 70 dpa/0.6 at.% He, corresponding to a full power service time of six months.

The main conclusions drawn from the present results and their discussion can be summarized as follows:

1. Micro-hardness, three-point bending and tensile tests gave consistent results showing irradiation hardening of high purity tantalum irradiated as target in ISIS.
2. Optical micrography after bending tests and even after bending end to end showed no cracks, indicating that Ta retained a very high ductility under 800 MeV proton irradiation.
3. This was confirmed by tensile tests at RT and 250 °C which showed that the strain-to-necking dropped from about 30% and 20% to about 10% and 8%,

[1] STIP stands for SINQ Target Irradiation Programme, an international collaboration using the Swiss Spallation Source as an irradiation facility.

respectively, after irradiation to 0.6 dpa, and then remained constant up to the maximum available dose of 11 dpa.
4. SEM investigation revealed typical ductile fracture surfaces even for the highest dose at test temperatures of 25 °C as well as 250 °C.
5. TEM investigations and simulation irradiations are under way to uncover the microstructural reason for the good resistance of pure tantalum against irradiation embrittlement.
6. Further irradiation experiments must prove that the high saturation ductility of around 10% is also maintained at very high dose levels.

Acknowledgements

The authors would like to thank Dr P. Jung for the useful discussions, and Dr M. Rödig for his help on temperature calibration of the tensile machine.

References

[1] ESS – A next generation neutron source for Europe, vol. III: The ESS Technical study, ESS Report 96-53-M, November 1996, ISBN 0902376500.
[2] H. Ullmaier, F. Carsughi, Nucl. Instrum. Meth. B 101 (1996) 406.
[3] F. Carsughi, H. Derz, P. Ferguson, G. Pott, W.F. Sommer, H. Ullmaier, J. Nucl. Mater. 264 (1999) 78.
[4] Y. Dai, F. Carsughi, W.F. Sommer, G. Bauer, H. Ullmaier, J. Nucl. Mater. 276 (2000) 289.
[5] J. Chen, Y. Dai, F. Carsughi, W.F. Sommer, G.S. Bauer, H. Ullmaier, J. Nucl. Mater. 275 (1999) 115.
[6] D. Filges, C. Mayr, R.D. Neef, H. Schaal, A. Tietz, J. Wimmer, ESS Report No. 96-45-T, 1996.
[7] S.L. Green, J. Nucl. Mater. 126 (1984) 30.
[8] S.L. Green, W.V. Green, F.H. Hegedus, M. Victoria, W.F. Sommer, B.M. Oliver, J. Nucl. Mater. 155–157 (1988) 1350.
[9] W.A. Coleman, T.W. Armstrong, Report ORNL-64606, Oak Ridge National Laboratory, USA, 1970.
[10] R.D. Brown, M.S. Wechsler, C. Tschalär, in: F.A. Garner, C.H. Henager, N. Igata (Eds.), Proccedings of the 13th International Symposium on Effects of Radiation on Materials Properties, ASTM STP 956, ASTM, Philadelphia, PA, 1987.
[11] F.W. Wiffen, in: R.J. Arsenault (Ed.), Proceedings of the 1973 International Symposium on Defect Clusters in B.C.C. Metals and Their Alloys, Washington, DC, 1973, p. 176.
[12] P.J. Ennis, M.E. Abd El-Azim, H. Schuster, in: E. Bachelet et al. (Eds.), High Temperature Materials for Power Engineering, Belgium, 1990, p. 143.
[13] M.R. James, M. Louthan, S.A. Maloy, W.F. Sommer, private communication, 1999.
[14] P. Jung, J. Henry, J. Chen, H. Klein, J.C. Brachet, W. Schmith, private communication.
[15] M.R. James, S.A. Maloy, F.D. Gac, W.F. Sommer, J. Chen, H. Ullmaier, J. Nucl. Mater. 296 (2001) 139.
[16] Tantalum, product description, Plansee GmbH, Austria.
[17] H. Trinkaus, H. Ullmaier, J. Nucl. Mater. 296 (2001) 101.